arXiv:hep-lat/0007035v1 24 Jul 2000

Cluster Percolation in O(n) Spin Models

P. Blanchard[1], S. Digal[1], S. Fortunato[1],
D. Gandolfo[2], T. Mendes[1], Helmut Satz[1]

[1] Fakultät für Physik, Universität Bielefeld, D-33615, Bielefeld, Germany.
[2] Dépt. de Math., Université de Toulon et du Var, , F-83957 La Garde Cedex,
& CPT, CNRS, Luminy, case 907, 13288 Marseille Cedex 09, FRANCE.

Abstract:

The spontaneous symmetry breaking in the Ising model can be equivalently described in terms of percolation of Wolff clusters. In O(n) spin models similar clusters can be built in a general way, and they are currently used to update these systems in Monte Carlo simulations. We show that for 3-dimensional O(2), O(3) and O(4) such clusters are indeed the physical 'islands' of the systems, i.e., they percolate at the physical threshold and the percolation exponents are in the universality class of the corresponding model. For O(2) and O(3) the result can be proven analytically, for O(4) it can be derived by numerical simulations.

1 Introduction

The possibility to interpret the critical behaviour of dynamical systems in terms of percolation of geometrical structures of the system has always had a great appeal in the study of critical phenomena [1] - [2]. Attempts in this direction were already done in the 70's, when one began to study the behaviour of clusters of nearest-neighbour like-signed spins in the Ising model. It turned out that in two dimensions these elementary site percolation clusters indeed undergo a geometrical transition exactly at the critical threshold of the Ising model [3]. This result, which is not valid in three dimensions [4], is anyway not so appealing, because the critical exponents derived by the percolation variables do not coincide with the Ising ones [5]. The correspondence between the geometrical and the thermal phenomenon is therefore only partial.

The problem was solved by A. Coniglio and W. Klein [2], making use of a different definition for the clusters. Such definition had already been used by Fortuin and Kasteleyn to show that the partition function of the Ising model can be rewritten in purely geometrical terms as a sum over clusters configurations [6]. According to the Fortuin-Kasteleyn prescription, two nearest-neighbouring spins of the same sign belong to the same cluster with a probability $p = 1 - exp(-2\beta)$ ($\beta = J/kT$, J is the Ising coupling). Coniglio and

Klein [2] showed that the geometrical transition of these clusters leads to the required critical indices of the Ising model, threshold and exponents.

The clusters of the Monte Carlo cluster update introduced by U. Wolff [7] for O(n) spin models coincide with the Fortuin-Kasteleyn ones when n=1 (which is just the Ising model). The O(n) models without external field in three space dimensions ($n \geq 2$) undergo a phase transition due to the spontaneous breaking of the continuous rotational symmetry of their Hamiltonian. Such models are very interesting: some physical systems in condensed matter physics are directly associated to them. The three-dimensional O(3) model is the low-temperature effective model for a bidimensional quantum antiferromagnet [8]. The O(2) model in three dimensions is known to be in the same universality class as superfluid ^4He. O(n) models are also very useful to study relativistic field theories. The O(4) model in three dimensions has been conjectured to be in the same universality class as the finite-temperature chiral phase transition of QCD with two flavours massless quarks [9].

The general definition of Wolff clusters for O(n) spin models inspired this work. Can one describe the critical behaviour of O(n) without field in three dimensions in terms of the percolation of these clusters, like in the case n=1? We will show that this is indeed true at least for O(2), O(3) and O(4). The fact that the Wolff clusters percolate at the physical critical point was recently proven analytically for O(2) and O(3) [10, 11]. Although nothing about the exponents was mentioned, we will show that starting from some relations established in [10, 11] it is also possible to deduce the equality of the critical exponents for O(2) and O(3). We have also performed computer simulations on O(2) and O(4) in order to illustrate this result for O(2), and to prove it numerically for O(4).

2 O(n) models and Wolff clusters

The O(n) spin models with no external magnetic field have the following Hamiltonian:

$$H = -J \sum_{\langle \mathbf{i},\mathbf{j} \rangle} \mathbf{s_i} \mathbf{s_j}, \tag{2.1}$$

where i and j are nearest-neighbour sites on a d-dimensional hypercubic lattice, and $\mathbf{s_i}$ is an n-component unit vector at site i (J is the coupling). The partition function of these models at the temperature T is

$$Z(T) = \int \mathcal{D}[\mathbf{s}] \exp\{\beta \sum_{\langle \mathbf{i},\mathbf{j} \rangle} \mathbf{s_i} \mathbf{s_j}\} \tag{2.2}$$

where $\beta = J/kT$ and the integral is extended over all spin configurations $\{\mathbf{s}\}$ of the system. In three dimensions the O(n) models undergo a second-order phase transition. The order parameter of this transition is the normalized magnetization $M = \frac{1}{V} \sum_{\mathbf{i}} \mathbf{s_i}$ (V is the lattice volume).

Numerical simulations of O(n) models became much quicker and more effective after U. Wolff [7] introduced a Monte Carlo algorithm based on simultaneous updates of large clusters of spins, generalizing the Swendsen Wang algorithm [12] to the continuous-spin case. This algorithm has the remarkable advantage that it eliminates the problem of

critical slowing down, an effect that makes simulations around criticality very lengthy with traditional local methods (Metropolis, heat bath). The Wolff algorithm can be basically divided in two phases:

1) a cluster of spins is selected;

2) the spins of this cluster are "flipped", i.e. they are reflected with respect to some defined hyperplane.

For details of the flipping procedure, see [7]. Here we are interested in the way to build up the clusters. We can split this procedure in two steps:

a) choose a random n-component unit vector $\mathbf{r}$;

b) bind together pairs of nearest-neighbouring sites i,j with the probability

$$p(i,j) = 1 - exp\{min[0, -2\beta(\mathbf{s_i}\cdot\mathbf{r})(\mathbf{s_j}\cdot\mathbf{r})]\}. \tag{2.3}$$

From this prescription it follows that if the two spins at two nearest-neighbouring sites i and j are such that their projections onto the random vector $\mathbf{r}$ are of opposite signs, they will never belong to the same cluster ($p(i,j) = 0$). The random vector $\mathbf{r}$, therefore, divides the spin space in two hemispheres, separating the spins which have a positive projection onto it from the ones which have a negative projection. The Wolff clusters are made out of spins which all lie either in the one or in the other hemisphere. In this respect, we can again speak of 'up' and 'down' spins, like for the Ising model. In addition to that, the bond probability is local, since it depends explicitly on the spin vectors $\mathbf{s_i}$ and $\mathbf{s_j}$, and not only on the temperature like the Fortuin-Kasteleyn factor.

The analogies with the Ising model are however clear, motivating the attempt to study the percolation properties of these clusters.

3 Percolation exponents for O(2) and O(3)

In [10, 11, 13] the random cluster representations of $O(n)$ models, $n = 2, 3$ have been derived (and exploited) through the Fortuin-Kasteleyn transformation [6] of the Hamiltonians and similar results were obtained in [14] for the continuous (or classical) spin model [15]. Wolff random cluster probability distributions [7] for these models have been studied and several monotonicity properties of these distributions (FKG properties) [16] have been established leading to the proof of the equivalence between the onset of magnetic ordering in the $O(n)$ models, $n = 2, 3$ and percolation in the corresponding random Wolff cluster models. From the results stated above follows in a natural way the equality of the critical thermal and geometrical exponents.

In what follows we focus our attention on two variables:

- The *percolation strength* P, defined as the probability that a lattice site picked up at random belongs to the percolating cluster. P is the *order parameter* of the percolation transition.

- The *average cluster size* S, defined as the average size of the non percolating clusters.

We stress that in some cases one speaks of average cluster size referring to the average size of *all* clusters, including the percolating one. This definition makes the variable

infinite above the percolation threshold. Below the threshold the two definitions obviously coincide and therefore they share the same critical exponent.

In the references [10, 11, 13, 14], it was proved that, if $P(T)$ is the percolation strength in the random Wolff cluster representation and $m(T)$ is the magnetization in the $O(n)$ spin system, then there exists a function $c(T) \in C^\infty(\mathbb{R}^+)$ such that

$$P(T) \geq m(T) \geq c(T)\ P(T) \tag{3.1}$$

Similarly, denoting $S(T)$ the average size of the Wolff clusters and $\chi(T)$ the (linear response) susceptibility, it was also proved that

$$S(T) \geq \chi(T) \geq c(T)^2 S(T) \tag{3.2}$$

where $c(T)$ is the same $C^\infty(\mathbb{R})$ function as in (3.1).

From scaling theory (see [17]), near criticality, the susceptibility is believed to behave according to the following law

$$\chi(T) \underset{T \to T_c^+}{\sim} (T - T_c)^{-\gamma} \tag{3.3}$$

and the average mean cluster size of Wolff clusters should follow the law

$$S(T) \underset{T \to T_c^+}{\sim} \mid p(T) - p(T_c) \mid^{-\gamma'} \tag{3.4}$$

where $p(T)$ is the bond occupation probability in the Wolff random cluster model (i.e. the Coniglio-Klein [2] bond probability) given by $p(T) \sim 1 - exp(-a/T)$, where a does not depend on T.

From [10, 11, 13, 14] the equality of the critical exponents γ and γ' follows readily . Indeed, because of monotonicity, taking the logarithm in (3.3) and (3.4), and using (3.2) one gets

$$-\gamma' \log \mid p(T) - p(T_c) \mid \geq -\gamma \log(T - T_c) \geq 2 \log c(T) - \gamma' \log \mid p(T) - p(T_c) \mid \tag{3.5}$$

which reduces to

$$\gamma' \geq \gamma\ \frac{\log(T - T_c)}{\log \mid p(T) - p(T_c) \mid} \geq \gamma' - \frac{2 \log c(T)}{\log \mid p(T) - p(T_c) \mid} \tag{3.6}$$

Now when $T \to T_c^+$ and since $c(T) \in C^\infty(\mathbb{R})$, the last term vanishes and it is easy to see that $\log(T - T_c)/\log \mid p(T) - p(T_c) \mid \underset{T \to T_c^+}{\to} 1$. When $T \to T_c^+$ we get the result $\gamma = \gamma'$.

Using (3.1) and the scaling behaviours of the magnetization and the percolation strength in terms of their critical exponents β and β' respectively, one can show (following the same lines as before) that $\beta = \beta'$ when $T \to T_c^+ \equiv p(T) \to p(T_c)^+$, where $p(T)$ is again the Coniglio-Klein bond probability already defined above.

Namely, the percolation strength is believed to behave [17] as a function of the elementary bond occupation probability p according to the following law

$$P(p) \underset{p \to p_c^+}{\sim} (p - p_c)^{\beta'} \qquad p \equiv p(T) \tag{3.7}$$

whereas, the magnetization should behave as

$$m(T) \underset{T\to T_c^-}{\sim} (T_c - T)^{\beta} \tag{3.8}$$

then using the same procedure as below, we are led to the following expression

$$\beta' \leq \beta \, \frac{\log(T_c - T)}{\log(p(T) - p(T_c))} \leq \beta' - \frac{\log c(T)}{\log(p(T) - p(T_c))} \tag{3.9}$$

which, using $\log(T_c - T)/\log(p(T) - p(T_c)) \underset{T\to T_c^-}{\to} 1$ and $\log c(T)/log(p(T) - p(T_c)) \underset{T\to T_c^-}{\to} 0$, gives

$$\beta = \beta'.$$

as claimed.

4 Numerical Results

We have investigated numerically the 3-dimensional O(2) and O(4) models performing computer simulations for several lattice sizes. The Monte Carlo update was performed by the Wolff algorithm, described in Section 2. At the end of an iteration, the percolation strength P and the average cluster size S were measured. This has been done for each of the models using two different approaches.

The **first approach** is the traditional one, based on a complete analysis of the lattice configuration. Once we have the configuration we want to analyze, we build Wolff clusters until all spins are set into clusters. We assign to P the value zero if there is no percolating cluster, the ratio between the size of the percolating cluster and the lattice volume otherwise. We calculate S using the formula

$$S = \sum_s \left(\frac{n_s s^2}{\sum_s n_s s} \right) . \tag{4.1}$$

Here n_s is the number of clusters of size s and the sums exclude the percolating cluster. The operative definition of percolating cluster was taken as follows. We say that a cluster percolates if it spans the lattice from a face to the opposite one in each of the three directions x, y, z. We made this choice to reduce the possibility that, due to the finite size of the lattices, one could find more than a spanning cluster making ambiguous the definition of our variables[1].

In this approach we have used free boundary conditions.

The **second approach** is based on a single-cluster analysis. Basically one studies the percolation properties of the cluster built during the update procedure. Since the probability of selecting a given cluster is proportional to its size, the definitions of P and S must differ from the ones used in the first method above. Let s_c be the size of

[1] In three dimensions even this definition of spanning cluster does not exclude the possibility of having more than one of such clusters for the same configuration. Nevertheless the occurrence of such cases is so small that we can safely ignore them.

this cluster. If it percolates we assign value one to the strength P and zero to the size S; otherwise, we write zero for P and ${s_c}^2$ for S. The observables thus described are equivalent to the ones used in the first approach, apart from normalization factors.

In this case we say that the cluster percolates if it connects at least one face with the opposite one. Since there can be only one spanning cluster in the infinite-volume limit [18], the two different definitions are not expected to affect the final results.

We have considered periodic boundary conditions for this approach.

The second approach has the advantage that it does not require a procedure to reduce the configuration of the system to a set of clusters; on the other hand, since it gets the information out of a single cluster, it requires a higher number of samples in order to measure the percolation variables with the same accuracy of the first method. Nevertheless, the iterations are faster due to the simpler measurement of observables, and are less correlated than in the first approach, since only a (random) limited region of the lattice is considered in each sample. We find that both methods are efficient, and that it is important to be able to compare results obtained in two such different ways.

For our numerical investigations we have also made use of another variable which can be extracted from the percolation strength P. On a finite lattice there is at any temperature β a well defined probability of having a spanning cluster. We call it percolation cumulant and indicate it γ_r. When the size of the lattice goes to infinity, γ_r as a function of β approaches a step function: it is always zero below β_c and always one above it. To get the finite-size curves out of our measurements we must basically see how often we found a percolating cluster ($P \neq 0$) for a definite lattice size and a temperature β.

To evaluate the thresholds and the exponents we have adopted finite-size-scaling techniques. We consider the general finite-size-scaling prediction for an observable $\mathcal{O}$

$$\mathcal{O}(t, L) \;=\; L^{\rho/\nu}\, Q_{\mathcal{O}}(L^{1/\nu} t)\;, \tag{4.2}$$

where $t = T - T_c$, L is the linear dimension of the lattice, $Q_{\mathcal{O}}$ is a universal function and the exponent ρ is related to the critical behavior of $\mathcal{O}$ at infinite volume. Following the definitions given in Section 3, we have $\rho = \gamma'$ for the observable S and $\rho = -\beta'$ for P. For the percolation cumulant γ_r we have $\rho = 0$ [17], which means that γ_r curves corresponding to different lattice sizes cross at the critical point: for $t = 0$ and $\rho = 0$, in fact, the observable of Eq. (4.2) is not L-dependent.

Figs. 1 and 2 show γ_r curves for O(2) and O(4), respectively. The agreement with the physical thresholds (dashed lines) is clear. Moreover, we could already get indications about the class of critical exponents of our clusters. In fact, if one knows the critical point and the exponent ν, a rescaling of γ_r as a function of $(T - T_c)L^{1/\nu}$ should give us the same function for each lattice size (see Eq. 4.2) . Figs. 3 and 4 show the rescaled percolation cumulant curves for O(2), using $\beta_c = 0.45416$ and two different values of the exponent ν, respectively the O(2) value and the random percolation one.

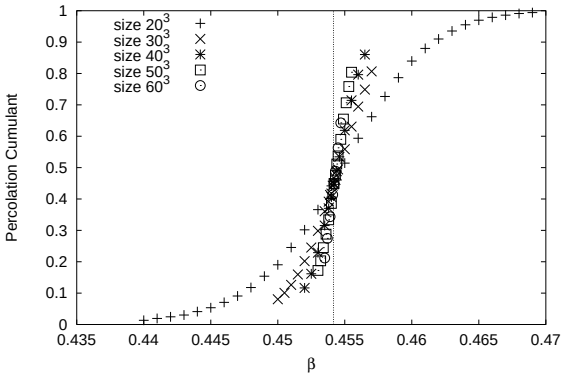

Figure 1. Percolation cumulant as function of β for O(2) and five lattice sizes. The dashed line indicates the position of the thermal threshold [19].

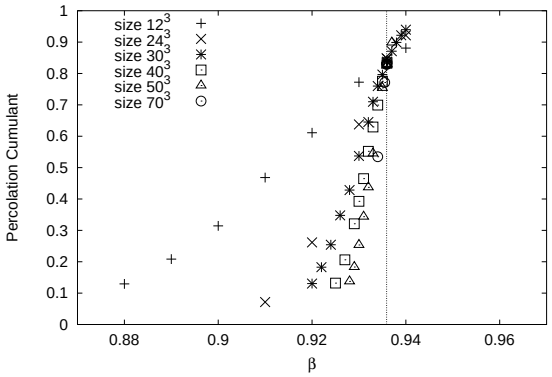

Figure 2. Percolation cumulant as function of β for O(4) and six lattice sizes. The dashed line indicates the position of the thermal threshold [20].

The scaling we get in correspondence of the O(2) value is remarkable. In Figs. 5 and 6 we repeat the same analysis for O(4) ($\beta_c = 0.9359$); also here it is clear that the percolation exponent ν is in agreement with the O(4) value. (We have considered values for the O(2) and O(4) models from Refs. [19] and [20, 21] respectively.)

To determine more precisely the critical point we have used the scaling relation (4.2) for the variables S and P. By plotting $\mathcal{O}$ as a function of L at the critical temperature, we can obtain the exponents' ratio ρ/ν directly from the slope of the data points in a log-log plot.

We concentrated ourselves on the critical regions that we localized through the percolation cumulant and performed more simulations for several β values looking for the β's for which we get the best χ^2 for the linear fit of the data points in a log-log plot. The results for O(2) and O(4) are in Tables I and II, respectively.

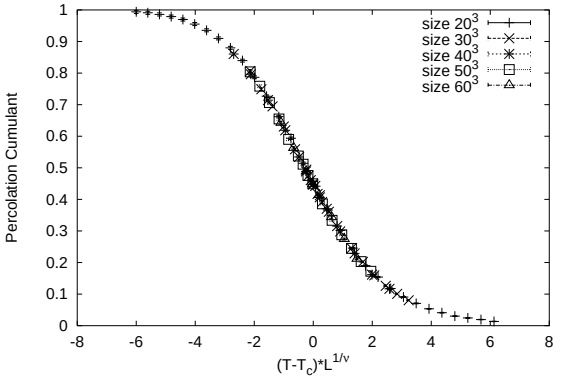

Figure 3. Rescaled percolation cumulant for O(2) using $\beta_c = 0.45416$ and the O(2) exponent $\nu = 0.672$.

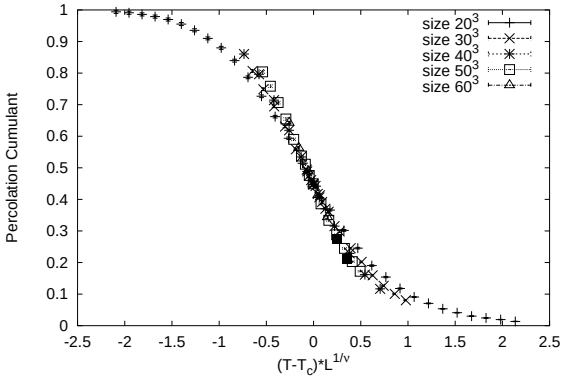

Figure 4. Rescaled percolation cumulant for O(2) using $\beta_c = 0.45416$ and the 3-dimensional random percolation exponent $\nu = 0.88$.

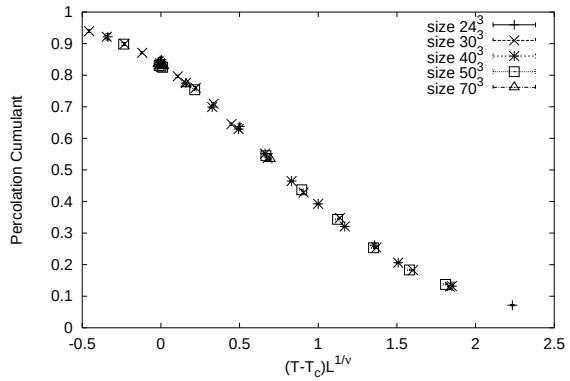

Figure 5. Rescaled percolation cumulant for O(4) using $\beta_c = 0.9359$ and the O(4) exponent $\nu = 0.742$.

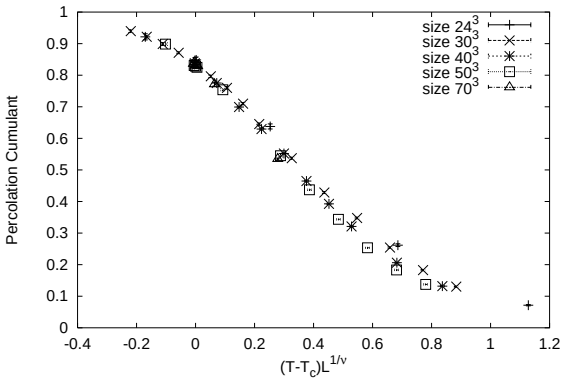

Figure 6. Rescaled percolation cumulant for O(4) using $\beta_c = 0.9359$ and the 3-dimensional random percolation exponent $\nu = 0.88$.

	β_c	β/ν	γ/ν
Percolation results	0.45418(2)	0.516(5)	1.971(15)
Thermal results [19]	0.454165(4)	0.5189(3)	1.9619(5)

Table I. Comparison of the thermal and percolation thresholds and exponents for O(2) .

	β_c	β/ν	γ/ν
Percolation results	0.93595(3)	0.515(5)	1.961(15)
Thermal results	0.93590(5)[20]	0.5129(11)[21]	1.9746(38)[21]

Table II. Comparison of the thermal and percolation thresholds and exponents for O(4).

The agreement with the physical values in Refs. [19, 20, 21] is good. So far we have presented the results obtained using the first approach. The results derived using the second approach are essentially the same; besides, we observe an improved quality of the scaling, mainly because of the use of periodic boundary conditions, which reduce

considerably the finite-size effects. In particular we show in Figs. 7, 8 the scaling of S and P at the thermal thresholds reported in Refs. [19, 20]. We observe very small finite-size effects (lattices of $L \geq 20$ are used in the fits), especially for the O(2) case, which is in contrast to what is observed for thermal observables [22]. The slopes of the straight lines are in agreement with the values of the thermal exponents' ratios β/ν, γ/ν.

We thus confirm numerically the equivalence found in Section 3 for the O(2) case, and verify that it holds also in the O(4) case.

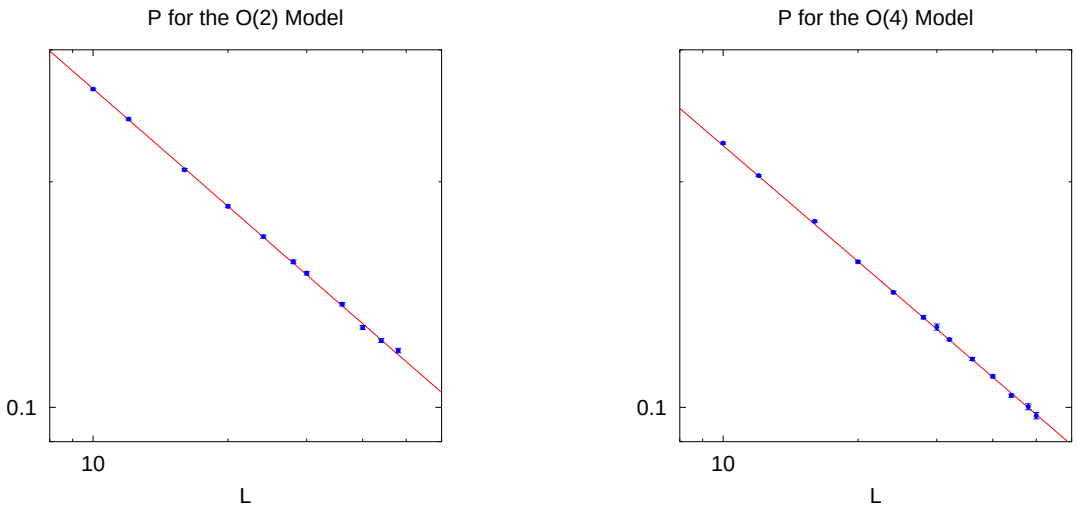

Figure 7: Finite-size-scaling plot at T_c for the percolation observable P as a function of the lattice size L. The slopes in the plots correspond to $\beta'/\nu' = 0.521(3), 0.513(6)$ respectively for O(2) and O(4). Error bars are one standard deviation.

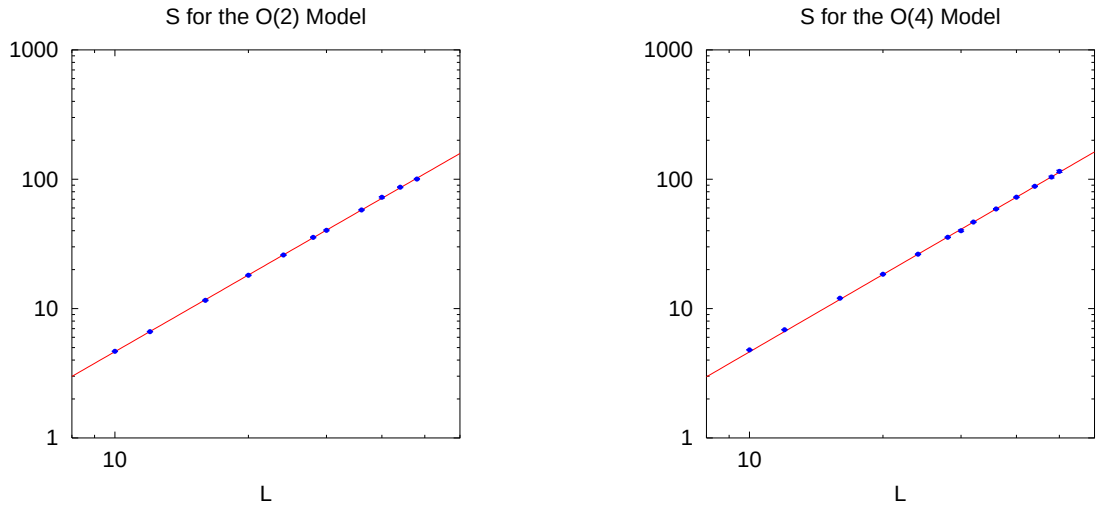

Figure 8: Finite-size-scaling plot at T_c for the percolation observable S as a function of the lattice size L. The slopes in the plots correspond to $\gamma'/\nu' = 1.97(1), 1.99(1)$ respectively for O(2) and O(4). Error bars are one standard deviation.

5 Conclusions

In this work we have shown that the spontaneous breaking of the continuous rotational symmetry for the 3-dimensional O(2), O(3) and O(4) spin models can be described as percolation of Wolff clusters. For O(2) and O(3) the result was proven analytically, for O(4) it was derived by means of lattice Monte Carlo simulations. In all cases, the number n of components of the spin vectors $\mathbf{s}$ does not seem to play a role; the result is thus likely to be valid for any O(n) model.

Acknowledgements

It is a pleasure to thank J. Engels for helpful discussions. We would also like to thank the TMR network ERBFMRX-CT-970122, the DFG Forschergruppe Ka 1198/4-1 and German Science Ministry BMBF under contract 06BI902 for financial support.

References

[1] M. E. Fisher, Physics **3**, 255-283 (1967).

[2] A. Coniglio, W. Klein, J. Phys. A. **13**, 2775 (1980).

[3] A. Coniglio et al., J. Physics A **10**, 205-218 (1977).

[4] H. Müller-Krumbhaar, Phys. Lett. A **48**, 459 (1974).

[5] M. F. Sykes, D. S. Gaunt, J. Phys. A **9**, 2131-2137 (1976).

[6] C. M. Fortuin, P. W. Kasteleyn, Physica **57**, 536 (1972).

[7] U. Wolff, Phys. Rev. Lett. **62**, 361 (1989).

[8] E. Manoussakis, R. Salvador, Phys. Rev. B **40**, 2205 (1989).

[9] R. Pisarski, F. Wilczeck, Phys. Rev. D **29**, 338 (1984); F. Wilczeck, Int. J. Mod. Phys. A **7**, 3911 (1992); K. Rajagopal, F. Wilczeck, Nucl. Phys. B **399**, 395 (1993).

[10] L. Chayes, Comm. Math. Phys. **197**, 623 (1998).

[11] M. Campbell, L. Chayes, J. Phys. A. **31**, 255-259 (1998).

[12] R. H. Swendsen, J. S. Wang, Phys. Rev. Lett. **58**, 86 (1987).

[13] P. Bialas et al., hep-lat/9911020, Nucl. Phys. B (in press).

[14] Ph. Blanchard, L. Chayes, D. Gandolfo, submitted to Nucl. Phys. B. (2000).

[15] R. B. Griffiths, J. Math. Phys. **10**, 1559 (1969).

[16] C. M. Fortuin, P. W. Kasteleyn, J. Ginibre, Comm. Math. Phys. **22**, 89 (1971).

[17] K. Binder, Monte Carlo Methods in Statistical Physics, Springer-Verlag (1986).

[18] C.M. Newman, L. S. Schulman, J. Stat. Phys. **26**, 613 (1981).

[19] M. Hasenbusch, T. Török, J. Phys. A **32**, 6361 (1999).

[20] M. Oevers, Diploma thesis, Bielefeld University (1996).

[21] K. Kanaya, S. Kaya, Phys. Rev. D **51**, 2404 (1995).

[22] J. Engels, T. Mendes, Nucl. Phys. B **572**, 289 (2000); J. Engels et al., hep-lat/0006023.

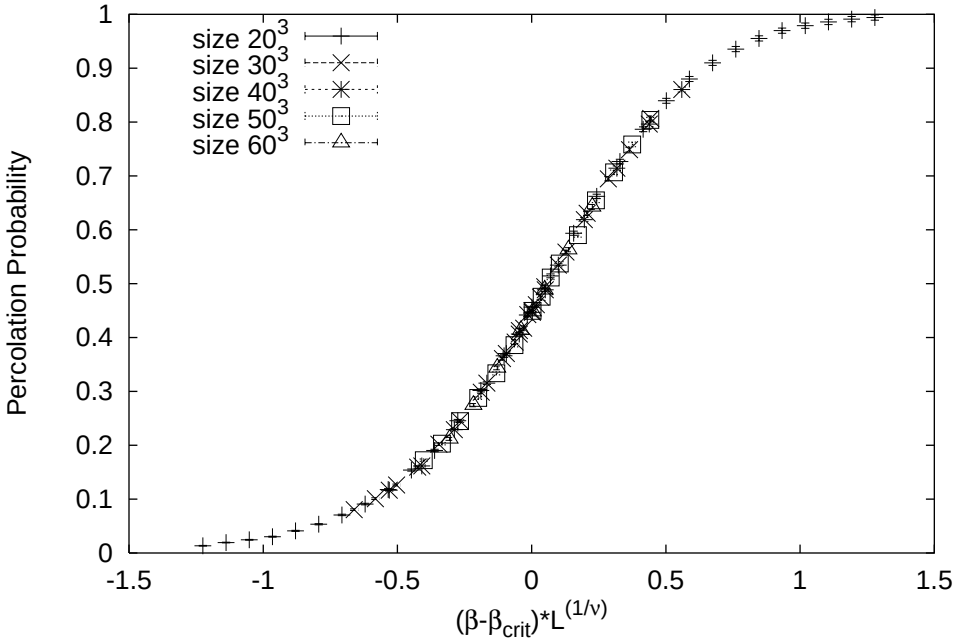
size 20^3
size 30^3
size 40^3
size 50^3
size 60^3
Percolation Probability
(β-β_crit)*L^(1/ν)
1
0.9
0.8
0.7
0.6
0.5
0.4
0.3
0.2
0.1
0
-1.5
-1
-0.5
0
0.5
1
1.5

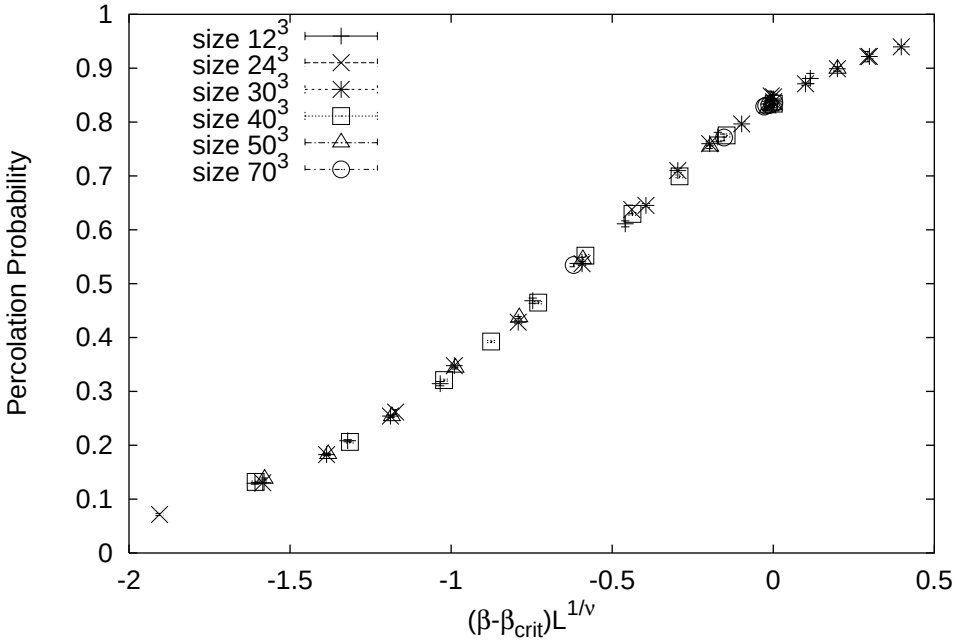
Percolation Probability
(β-β_crit)L^1/ν
size 12^3
size 24^3
size 30^3
size 40^3
size 50^3
size 70^3
0
0.1
0.2
0.3
0.4
0.5
0.6
0.7
0.8
0.9
1
-2
-1.5
-1
-0.5
0
0.5